Magnetic structures of the three-dimensional Heisenberg antiferromagnets $K_2FeCl_5.D_2O$ and $Rb_2FeCl_5.D_2O$

1995 J. Phys.: Condens. Matter 7 4725

(http://iopscience.iop.org/0953-8984/7/24/012)

J. Phys.: Condens. Matter 7 (1995) 4725–4738. Printed in the UK

Magnetic structures of the three-dimensional Heisenberg antiferromagnets $K_2FeCl_5 \cdot D_2O$ and $Rb_2FeCl_5 \cdot D_2O$

M Gabás†, F Palacio†, J Rodríguez-Carvajal‡§ and D Visser‖

† Instituto de Ciencia de Materiales de Aragón, CSIC—Universidad de Zaragoza, E-50009 Zaragoza, Spain

‡ Laboratoire Leon Brillouin (CEA-CNRS), Centre de Saclay, 91191 Gif sur Yvette Cédex, France

§ Institut Laue Langevin, BP 156X, F-38042 Grenoble Cédex, France

‖ Department of Physics, Loughborough University of Technology, Loughborough, UK

Received 11 January 1995

Abstract. The crystal and magnetic structures of $K_2FeCl_5 \cdot D_2O$ and $Rb_2FeCl_5 \cdot D_2O$ have been determined by neutron powder diffraction. The crystal structure of $K_2FeCl_5 \cdot H_2O$ has been redetermined using single-crystal diffraction. All compounds crystallize with the orthorhombic space group *Pnma*. The magnetic structure of both deuterated compounds can be described by ferromagnetic planes perpendicular to the b axis coupled antiferromagnetically to each other. The critical behaviour of the staggered magnetization below $T_N = 14.2$ K and 10.0 K for $K_2FeCl_5 \cdot D_2O$ and $Rb_2FeCl_5 \cdot D_2O$, respectively, can be described by a power law for reduced temperature $0.03 < t < 0.2$ by a critical exponent $\beta = 0.35 \pm 0.02$.

1. Introduction

The compounds $A_2FeX_5 \cdot H_2O$, where A = Cs, Rb, NH_4, K and X = Cl, Br, form a series of easy-axis antiferromagnets (Carlin and Palacio 1985). Their low magnetic anisotropy is due to the high-spin state ($S = \frac{5}{2}$) of the Fe(III) ions. The ratio between the anisotropy field and the exchange field, $\alpha = H_A/H_E$, as calculated from the magnetic phase diagrams is rather low for these compounds, e.g. $\alpha = 8.5 \times 10^{-3}$ and 3.4×10^{-3} for, respectively, $K_2FeCl_5 \cdot H_2O$ (Palacio *et al* 1980) and $Rb_2FeCl_5 \cdot H_2O$ (O'Connor *et al* 1979). The crystallographic structure contains discrete $[FeX_5(H_2O)]^{2-}$ octahedra that are connected by hydrogen bonding. Except for $Cs_2FeCl_5 \cdot H_2O$, which crystallizes with the *Cmcm* space group, all the other compounds are isomorphous and crystallize in the *Pnma* space group (Carlin and Palacio 1985).

The magnetic structures of these $A_2FeCl_5 \cdot D_2O$-type compounds are investigated to confirm the predictions made from magnetic susceptibility and specific heat and as a basis for the interpretation of the novel magnetic behaviour observed in the diamagnetically doped $A_2Fe_{1-x}In_xCl_5 \cdot H_2O$ systems.

The magnetic properties of the Rb, K and NH_4 chlorine derivatives were first interpreted in terms of the presence of coupled antiferromagnetic linear chains (McElearney and Merchant 1978, O'Connor *et al* 1979). A more detailed study of the magnetic properties showed that the heat capacity and low-temperature magnetic susceptibility data can be better explained assuming a lattice dimensionality crossover in a Heisenberg model where exchange interaction is about ten times stronger along one direction of the crystal lattice than in the others (Puértolas *et al* 1985).

0953-8984/95/244725+14$19.50

The magnetic ordering temperatures, T_N, exhibited by these compounds range between 5 and 25 K. They are in sharp contrast to the values below 1 K typically observed in other double-salt hydrates. Superexchange pathways connecting the metal ions involve more than one diamagnetic bridging atom, such as Fe–X···X–Fe and Fe–O–H···X–Fe, and the presence of hydrogen bonds seems to play an important role in the enhancement of the magnetic interactions (Puértolas *et al* 1982, 1985). It is therefore of interest to determine the positions of the H atoms in the lattice and to clarify their role in the transmission of the magnetic interactions.

An anomalous remanent magnetization has recently been observed at very low magnetic fields in diluted samples of $A_2Fe_{1-x}In_xCl_5 \cdot H_2O$, where A = Rb and K (Paduan-Filho *et al* 1992, Becerra *et al* 1994, Palacio *et al* 1994), and the nuclear structures of $A_2MCl_5 \cdot H_2O$ (A = K, Rb; M = Fe, In) are all isomorphous (Carlin and Palacio 1985, Wignacourt *et al* 1976, Solans *et al* 1988). Anomalies of the same type have also been observed in other diluted low-anisotropy antiferromagnets (Lederman *et al* 1990, Fries *et al* 1993a, b, Kushauer *et al* 1994). After appropriate normalization the experimental values of such remanent magnetization corresponding to a rather large variety of solid solutions have been found to collapse in a unique universal curve (Palacio *et al* 1994). While the remanence in the $A_2Fe_{1-x}In_xCl_5 \cdot H_2O$ is well established and characterized, its origin is still unclear. Magnetization in the bulk of a domain due to the piezomagnetic effect has been suggested as a possibility (Kushauer *et al* 1994). Such a piezomagnetic effect was observed in crystals of MnF_2 as a shift in the magnetization curve when measured parallel to the easy axis in the presence of hydrostatic pressure (Borovik-Romanov 1960). In the case of a disordered antiferromagnet it has been argued that the random built-in stress field caused by the lattice distortion would result in a local decompensation at the sublattice magnetization. At zero magnetic field there would be no preferred direction for the alignment of such local decompensation in the magnetic lattice other than the easy axis within each antiferromagnetic domain. However, these tiny magnetic moments would tend to align in the presence of a quite weak magnetic field thus yielding a remanent moment to the antiferromagnetic lattice. This argument has been used to explain the remanent magnetization observed in crystals of $Mn_{1-x}Zn_xF_2$, on the basis that the magnetic class of MnF_2 is $4'/mmm'$ (Erickson 1953) which allows piezomagnetism. Independent of the adequacy of arguing on the presence of piezomagnetism in a disordered system, it would be of interest to know whether the magnetic space group of $A_2FeCl_5 \cdot D_2O$ (A = K, Rb) can sustain this phenomenon. The determination of these magnetic structures might, therefore, contribute to understanding of the anomalous magnetic remanence described above.

2. Experimental section

Polycrystalline samples of $K_2FeCl_5 \cdot D_2O$ and $Rb_2FeCl_5 \cdot D_2O$ were prepared by grinding up small single crystals of these materials. The crystals were grown following a method already described (Linke 1965).

Neutron diffraction experiments were performed at the high-flux reactor of the Institut Laue–Langevin in Grenoble (France). Each sample was placed into a cylindrical vanadium can (d = 8 mm, h = 50 mm) and inserted into a helium cryostat working in a temperature range between 1.5 and 330 K. The temperature was computer controlled and its stability during the measurements was better than 0.1 K.

For the purpose of structural refinement, diffraction patterns at several temperatures (room temperature (RT), 80, 20 and 1.6 K for $K_2FeCl_5 \cdot D_2O$ and RT, 100, 20 and 1.6 K for $Rb_2FeCl_5 \cdot D_2O$) were collected in the high resolution neutron powder diffractometer D2B

Table 1. Structural parameters and agreement factors for $K_2FeCl_5 \cdot H_2O$ (x-ray data).

	x/a	y/b	z/c	U_{11}	U_{22}	U_{33}	U_{12}	U_{13}
K	0.354 68(6)	0.498 82(7)	0.146 5(1)	0.040 0(5)	0.037 8(5)	0.041 2(6)	0.000 1(3)	0.006 3(3)
Fe	0.114 57(4)	0.250 00	0.190 24(8)	0.019 15(4)	0.018 02(4)	0.020 97(4)	0.000 0	−0.003 4(2)
Cl1	0.250 19(7)	0.250 00	0.392 3(2)	0.023 8(5)	0.031 4(6)	0.024 1(6)	0.000 0	−0.006 2(3)
Cl2	0.217 9(1)	0.250 00	−0.079 4(2)	0.045 1(7)	0.046 5(6)	0.022 40(7)	0.000 0	0.006 9(5)
Cl3	0.005 97(8)	0.250 00	0.458 7(2)	0.029 4(6)	0.038 3(6)	0.037 6(6)	0.000 0	0.012 0(4)
Cl4	0.104 93(7)	0.493 74(8)	0.180 9(1)	0.040 9(6)	0.017 6(5)	0.044 8(6)	−0.000 3(2)	−0.013 9(3)
O	0.006 4(2)	0.250 00	0.008 9(5)	0.029(1)	0.021(1)	0.054(2)	0.000 0	−0.026(1)
H	−0.004 4(30)	0.312 6(33)	−0.037 2(57)	0.058(11)[a]				
	a (Å)	b (Å)	c (Å)	R (%)	R_w (%)			
	13.579 5(7)	9.702 4(7)	7.014 7(3)	3.91	3.76			

[a] Anisotropic temperature factors, U_{ij}, are given for all the atoms but hydrogen, where an isotropic factor is provided.

($\lambda = 1.5945$ Å) using its high-flux mode of operation. The bank of 64 detectors, separated 2.5° in 2θ, was moved in steps of 0.05° to cover a total angular range of $5° \leqslant 2\theta \leqslant 160°$. Additional data at RT was collected for $Rb_2FeCl_5 \cdot D_2O$ in the high resolution powder diffractometer D1A ($\lambda = 1.909$ Å), the bank of 10 detectors covering an angular range of 60°, but when displaced, covers a total range $2° \leqslant 2\theta \leqslant 150°$.

The magnetically ordered phases were studied in the medium-resolution neutron powder diffractometer D1B ($\lambda = 2.52$ Å), which has a position sensitive detector (PSD) with 400 cells separated by a step width of 0.2° in 2θ; the total angular range covered is 80°. The good resolution at small angles and the high neutron flux make D1B very suitable to follow the thermal evolution of the magnetic reflections. The diffraction patterns were collected scanning the temperature between 1.5 and 26.55 K for $Rb_2FeCl_5 \cdot D_2O$, and between 1.5 and 18.2 K for $K_2FeCl_5 \cdot D_2O$, in the angular range $5° \leqslant 2\theta \leqslant 85°$. Data were analysed using the program FULLPROF (Rodríguez-Carvajal 1990, 1993), which allows the refinement of multiphase pattern, magnetic structures and anisotropic broadening of reflections.

The room-temperature structure of $K_2FeCl_5 \cdot D_2O$ was determined from single-crystal x-ray diffraction. Measurements were performed in a Siemens/Stoe AED2 four-circle diffractometer: $\lambda = 0.71073$ Å, μ(Mo Kα) = 3.90 mm^{-1}. A total of 985 reflections were collected in the angular range $4° \leqslant 2\theta \leqslant 50°$ from which 763 with $F_0^2 \geqslant 3\sigma(F_0^2)$ were selected for structure refinement; the weighting scheme was $w^{-1} = \sigma(F_0) + 0.022\,721(F_0^2)$. No absorption correction was made. All atoms were treated as anisotropic except the hydrogen atom. Unit cell parameters were refined using 27 selected reflections. The extinction conditions were consistent with the space group *Pnma*. Data were analysed in a VAX cluster (VAX/VMS V5.5) with the program REDU4 rev 7.03 (Stoe) for data reduction and the program package SHELXTL-PLUS release 4.21/V (©1990, Siemens Analytical X-ray Instruments, Inc., Madison, Wisconsin).

3. Results and discussion

3.1. Nuclear structures of $K_2FeCl_5 \cdot H_2O$ and $K_2FeCl_5 \cdot D_2O$

The single-crystal data allowed to refine the structure of $K_2FeCl_5 \cdot H_2O$ initially described by Bellanca (1948) and to determine the positions of the hydrogen atoms. Refined structural parameters are given in table 1.

The spatial arrangement of the atoms consists of octahedra where five chlorines and the oxygen atom are placed at the corners and the Fe atom at the centre (figure 1). In each octahedron the iron atom, three chlorines and the oxygen occupy a special position 4c, with point symmetry *m*. The other two chlorines and the K atoms are in a general position. The octahedra are arranged in planes perpendicular to the *b* axis. For each octahedron, the hydrogen atoms are placed each on one side of the symmetry plane. The octahedra are slightly distorted because of the different iron–chlorine and iron–oxygen bond lengths.

The nuclear structure of $K_2FeCl_5 \cdot D_2O$ was determined from neutron powder diffraction data collected on D2B. Some extra peaks due to a small impurity of KCl were observed in the diffraction patterns. The nuclear structure was refined from data obtained at RT, 80 and 20 K. An additional refinement at 1.6 K was made together with the determination of the magnetic structure. For each temperature the refined structural parameters are given in table 2. The observed and calculated patterns at 80 K are shown in figure 2(a). No structural differences have been observed between this compound and the undeuterated one, nor have structural changes been detected as the sample was cooled from RT down to 1.6 K apart from small variations of the atomic positions. Lists of the most relevant distances and bond

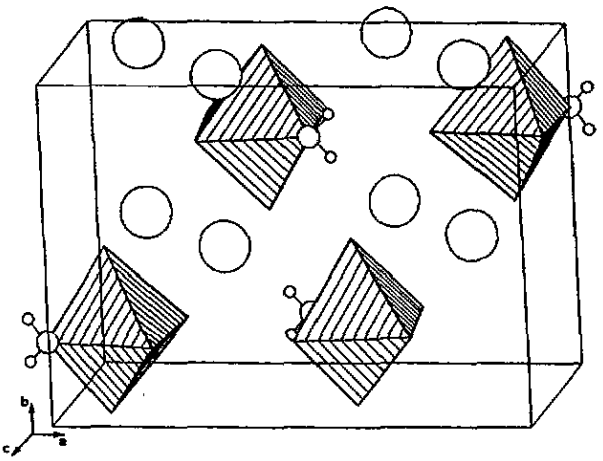

Figure 1. The unit cell contents of $K_2FeCl_5 \cdot H_2O$, showing the $[FeCl_5(H_2O)]^{2-}$ octahedra. The larger circles are K^+ cations, while the H_2O molecules constituting part of the octahedra are emphasized.

Table 2. Structural parameters and agreement factors for $K_2FeCl_5 \cdot D_2O$ (neutron data) at four temperatures.

T (K)		K	Fe	Cl1	Cl2	Cl3	Cl4	O	D
300		0.3502(10)	0.1150(6)	0.2466(6)	0.2213(7)	0.0042(6)	0.10605(4)	−0.0063(12)	−0.0372(7)
80		0.3546(6)	0.1157(4)	0.2501(4)	0.2201(4)	0.0060(4)	0.1046(2)	−0.0101(7)	−0.0355(5)
20	x/a	0.3535(7)	0.1158(4)	0.2512(4)	0.2197(4)	0.0069(4)	0.1048(2)	−0.0083(7)	−0.0363(4)
1.6		0.3536(7)	0.1154(4)	0.2516(4)	0.2197(4)	0.0070(4)	0.1049(2)	−0.0079(7)	−0.0364(4)
300		0.5125(23)	0.2500	0.2500	0.2500	0.2500	0.4907(6)	0.2500	0.3315(11)
80		0.4947(14)	0.2500	0.2500	0.2500	0.2500	0.4957(4)	0.2500	0.3326(7)
20	y/b	0.4947(14)	0.2500	0.2500	0.2500	0.2500	0.4958(4)	0.2500	0.3325(7)
1.6		0.4970(14)	0.2500	0.2500	0.2500	0.2500	0.4961(4)	0.2500	0.3324(7)
300		0.1357(20)	0.1917(13)	0.3870(12)	−0.0847(12)	0.4512(12)	0.1785(79)	0.0151(24)	−0.0450(15)
80		0.1430(11)	0.1953(8)	0.3919(7)	−0.0799(7)	0.4655(7)	0.1862(4)	0.0230(12)	−0.048(11)
20	z/c	0.1418(12)	0.1954(8)	0.3943(7)	−0.0800(7)	0.4678(6)	0.1867(4)	0.0237(11)	−0.0477(9)
1.6		0.1409(12)	0.1950(8)	0.3947(7)	−0.0802(7)	0.4678(7)	0.1866(4)	0.0239(12)	−0.04767(9)

	a (Å)	b (Å)	c (Å)	R_{Bragg} (%)	R_{wp} (%)	R_{exp} (%)	m (μ_B)
300	13.5862(9)	9.7087(5)	7.0177(5)	11.5	17.8	3.27	
80	13.4653(3)	9.6132(2)	6.9836(2)	10.7	18.8	2.86	
20	13.4389(3)	9.6025(2)	6.9789(2)	11.2	8.75	1.19	
1.6	13.4391(3)	9.5981(2)	6.9797(2)	11.1	19.7	2.93	3.9(1)

angles are given in tables 3 and 4. These results are in good agreement with those obtained at ambient pressure in a very recent study of the structural dependence of this compound on hydrostatic pressure (Schultz and Carlin 1995).

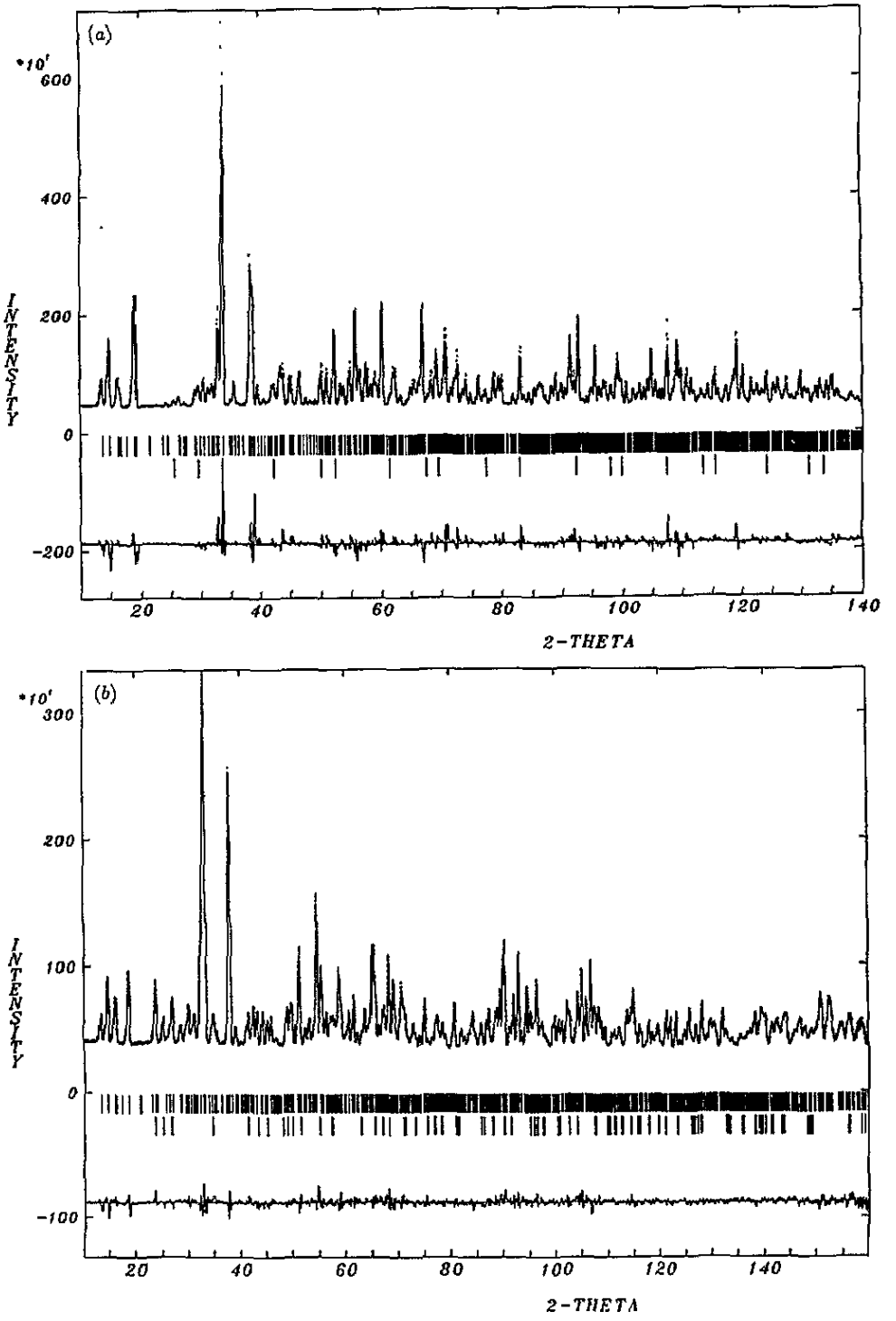

Figure 2. Observed (dotted curve) and calculated (full curve) patterns of (a) $K_2FeCl_5 \cdot D_2O$ at 80 K, and (b) $Rb_2FeCl_5 \cdot D_2O$ at 100 K. The difference pattern is given at the bottom of the figures on the same scale. Angular positions of the allowed Bragg reflections are indicated by small bars. The second row of bars corresponds to the reflections arising from an impurity (see text).

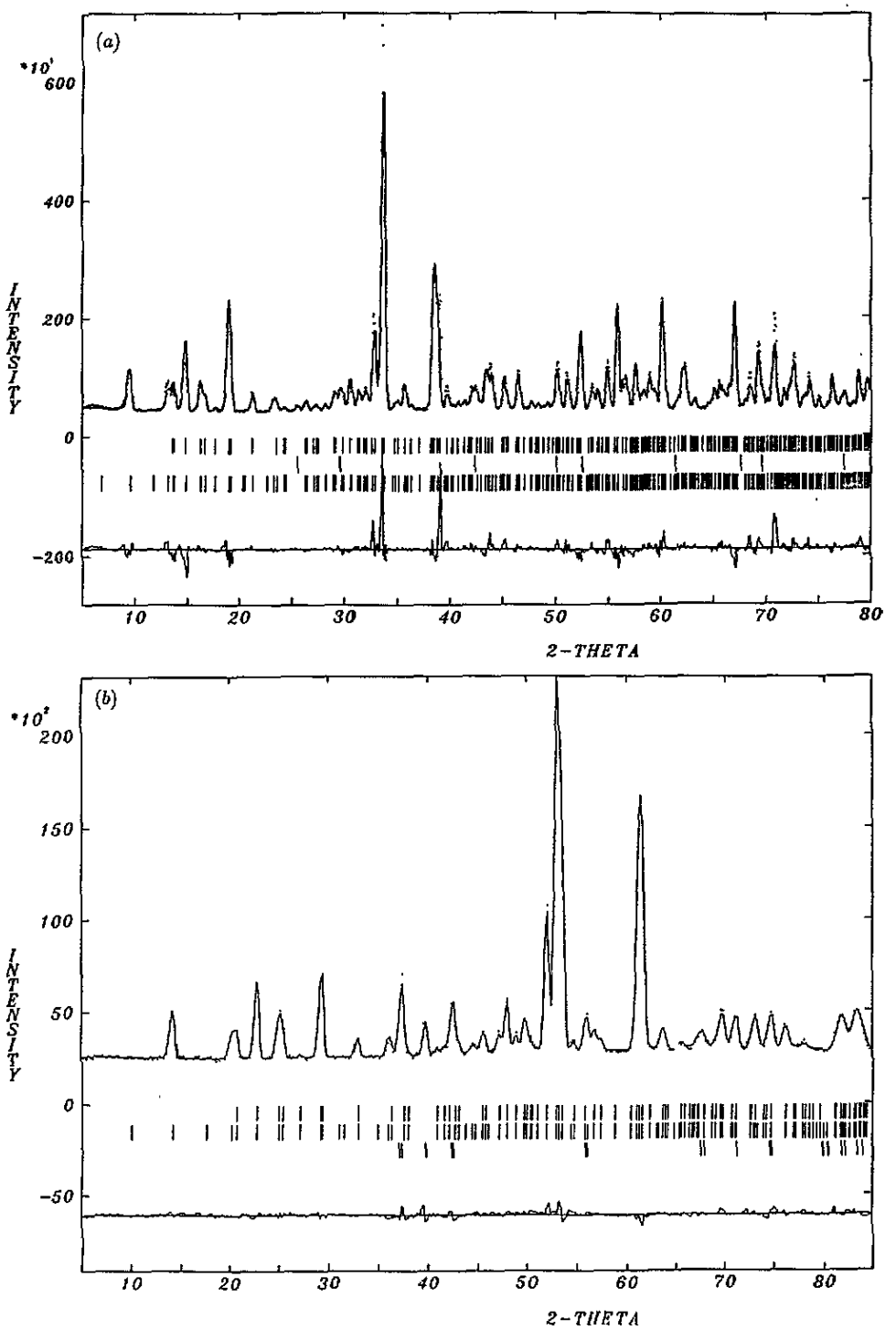

Figure 3. Observed (dotted curve) and calculated (full curve) nuclear and magnetic intensities at 1.5 K of (a) $K_2FeCl_5 \cdot D_2O$, and (b) $Rb_2FeCl_5 \cdot D_2O$. The first row of vertical bars denotes the positions of possible nuclear reflections, the second row denotes the positions of lines from an impurity phase and the third row denotes the positions of possible nuclear and magnetic reflections (see text).

Table 3. Bond length (Å) for $K_2FeCl_5 \cdot H_2O$ at room temperature. Distances between atoms from different $[FeCl_5(H_2O)]^{2-}$ clusters but participating in superexchange pathways are also included. The superexchange path is indicated with roman numerals.

Fe–Cl1	2.324(1)	Fe–Cl2	2.355(1)
Fe–Cl3	2.392(1)	Fe–Cl4	2.369(1)
Fe–O	2.078(4)	O–H	0.861(37)
Cl4....I....H	2.288(35)	Fe....I....Fe	6.351 3(7)
Cl1...II...H	3.032(41)	Fe...II...Fe	6.841 6(5)
Cl3...III...H	3.592(34)	Fe...III...Fe	7.015 0(1)
Cl4..IV..Cl4	3.818(2)	Fe...IV...Fe	7.026 0(7)

Table 4. Bond angles (deg) for $K_2FeCl_5 \cdot H_2O$ at room temperature.

Cl1–Fe–Cl2	91.0(0)
Cl1–Fe–Cl3	90.5(0)
Cl1–Fe–Cl4	93.5(0)
Cl1–Fe–O	179.8(3)
Cl2–Fe–Cl3	178.5(1)
Cl2–Fe–Cl4	90.6(0)
Cl2–Fe–O	88.8(1)
Cl3–Fe–Cl4	89.3(0)
Cl3–Fe–O	89.7(1)
Cl4–Fe–O	86.5(0)
Fe–O–H	135(2)

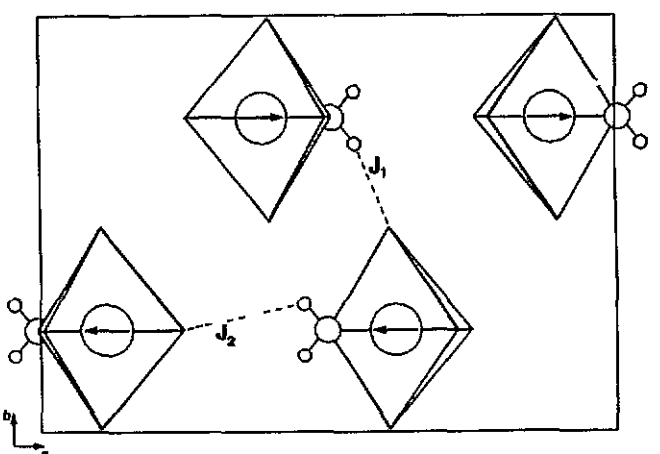

Figure 4. Projection of the unit cell of $Rb_2FeCl_5 \cdot D_2O$ and $K_2FeCl_5 \cdot D_2O$ along [001], showing the orientation of the magnetic moments. Rb/K atoms are not shown for clarity. Broken lines identify superexchange pathways.

3.2. Nuclear structure of $Rb_2FeCl_5 \cdot D_2O$

The structure of this compound, isomorphous with that of the K derivative (O'Connor *et al* 1979), has been refined from neutron powder diffraction data collected on D2B at RT, 100 K and 20 K. This has allowed the positions for the deuterium atoms to be determined. The observed and calculated patterns at 100 K are shown in figure 2(b); at this temperature,

Table 5. Structural parameters and agreement factors for $Rb_2FeCl_5 \cdot D_2O$ (neutron data) at four temperatures.

T (K)	Rb	Fe	Cl1	Cl2	Cl3	Cl4	O	D	
300		0.3565(2)	0.1155(2)	0.2452(2)	0.2203(3)	0.0063(3)	0.1040(1)	−0.0064(6)	−0.0345(4)
100		0.3569(1)	0.1150(1)	0.2471(1)	0.2234(1)	0.0053(1)	0.1040(0)	−0.0042(3)	−0.0343(1)
20	x/a	0.3567(1)	0.1149(2)	0.2462(2)	0.2236(2)	0.0066(2)	0.1032(1)	−0.0020(4)	−0.0342(2)
1.6		0.3566(1)	0.1147(2)	0.2464(2)	0.2238(2)	0.0066(2)	0.1032(1)	−0.0014(4)	−0.0341(2)
300		0.5003(6)	0.2500	0.2500	0.2500	0.2500	0.4902(2)	0.2500	0.3298(6)
100		0.4989(3)	0.2500	0.2500	0.2500	0.2500	0.4919(1)	0.2500	0.3300(2)
20	y/b	0.4987(4)	0.2500	0.2500	0.2500	0.2500	0.4907(2)	0.2500	0.3294(3)
1.6		0.4992(4)	0.2500	0.2500	0.2500	0.2500	0.4907(2)	0.2500	0.3297(4)
300		0.1554(5)	0.1916(5)	0.3988(4)	−0.0697(5)	0.4527(5)	0.1768(3)	0.0034(11)	−0.0450(9)
100		0.1606(2)	0.1936(2)	0.4018(2)	−0.0689(2)	0.4595(2)	0.1799(2)	0.0110(5)	−0.0488(3)
20	z/c	0.1594(4)	0.1931(4)	0.4027(4)	−0.0670(4)	0.4623(4)	0.1797(2)	0.0124(8)	−0.0483(5)
1.6		0.1599(4)	0.1936(4)	0.4023(4)	−0.0665(4)	0.4622(4)	0.1794(3)	0.0122(8)	−0.0479(5)

	a (Å)	b (Å)	c (Å)	R_{Bragg} (%)	R_{wp} (%)	R_{exp} (%)	m (μ_B)
300	13.8015(2)	9.9049(1)	7.0783(1)	7.31	11.1	6.76	
100	13.7101(1)	9.8517(1)	7.0255(0)	4.95	9.77	4.29	
20	13.6798(2)	9.8507(2)	7.0069(1)	5.66	10.9	2.87	
1.6	13.6801(2)	9.8471(2)	7.0073(1)	5.93	11.3	2.87	4.06(5)

extra peaks from an impurity of D_2O are observed in the diffractogram. An additional refinement at 1.6 K was made together with the determination of the magnetic structure. The refined structural parameters at every temperature are given in table 5. The only structural differences observed with the potassium derivative come from the different radii of the K^+ and Rb^+ ions that modify slightly the unit cell sizes and atom positions. No structural changes were detected as the sample was cooled from room temperature down to 1.6 K. It is noteworthy that this is not the case in other closely related compounds such as $Cs_2FeCl_5D_2O$ and $(NH_4)_2FeCl_5D_2O$. In the first, a structural change occurs between RT and 77 K (Johnson *et al* 1987), while in the second a rather complicated pattern of phases is observed in the neutron diffraction patterns in the temperature region around 125 K (Palacio and Visser 1995). In tables 6 and 7, some relevant distances and bond angles are shown.

Table 6. Selected bond lengths (Å) for $Rb_2FeCl_5 \cdot D_2O$ at 1.6 K. Data collected in D2B. Significant distances in superexchange pathways are also included. The superexchange path is indicated with roman numerals.

Fe–Cl1	2.321(5)	Fe–Cl2	2.356(4)
Fe–Cl3	2.394(4)	Fe–Cl4	2.378(2)
Fe–O	2.035(7)	O–D	0.998(6)
Cl4....I....D	2.206(5)	Fe....I....Fe	6.439(4)
Cl1...II...D	3.266(5)	Fe...II...Fe	6.8855(7)
Cl3...III...D	3.565(5)	Fe...III...Fe	7.0073(1)
Cl4..IV..Cl4	3.788(4)	Fe...IV...Fe	7.086(3)

Table 7. Selected bond angles (deg) for $Rb_2FeCl_5 \cdot D_2O$ at 1.6 K. Data collected in D2B.

Cl1–Fe–Cl2	89.8(3)
Cl1–Fe–Cl3	89.1(2)
Cl1–Fe–Cl4	94.45(9)
Cl1–Fe–O	179.6(2)
Cl2–Fe–Cl3	178.9(2)
Cl2–Fe–Cl4	90.54(9)
Cl2–Fe–O	90.6(2)
Cl3–Fe–Cl4	89.55(9)
Cl3–Fe–O	90.5(2)
Cl4–Fe–O	85.55(9)
Fe–O–D	127.9(4)

3.3. Magnetostructural correlations

Superexchange pathways were identified in these compounds by Puértolas and co-workers (1985). They proposed four different pathways, all involving two non-magnetic atoms. The knowledge of the hydrogen positions permits us now to corroborate the former identification. The most intense path, labelled J_1, would go through mixed oxygen–hydrogen–chlorine bridges, using the hydrogen bond to propagate the interaction, forming zig-zag chains parallel to the *b* axis (figure 4). This interaction should be the strongest since it shows the minimum Cl...D distance (2.206(5) Å). The second and third interactions, J_2 and J_3, propagate also through oxygen–hydrogen–chlorine bridges but in directions parallel to *a* and *c* axes respectively. Both connect spins which are ferromagnetically coupled and they are weaker than J_1. Pathway interaction J_2 is shown in figure 4; the Cl...D distance here is bigger (3.266(5) Å) than the corresponding one to J_1. The fourth interaction, J_4, does not involve hydrogen atoms and it propagates through chlorine–chlorine bridges connecting iron atoms from neighbouring ferromagnetic planes. Since the Fe–Cl bond is longer than the Fe–O bond, J_4 is the weakest interaction in the magnetic system.

3.4. Magnetic structures

No large differences are observed in the diffraction patterns of $K_2FeCl_5 \cdot D_2O$ and $Rb_2FeCl_5 \cdot D_2O$ collected at 1.5 K. This indicates that the magnetic structures of these compounds are essentially equal. Since all the magnetic reflections can be indexed in the nuclear cell, the propagation vector of the magnetic structure is $k = (0, 0, 0)$. Using Bertaut's macroscopic theory (Bertaut 1968) the eight irreducible representations of the space group *Pnma* for $k(0, 0, 0)$ and the basis functions corresponding to the position 4c occupied by Fe ions have been calculated. According to previously reported magnetic measurements (Carlin and Palacio 1985 and references therein), these compounds are collinear antiferromagnets with the easy axis aligned parallel to the *a* crystallographic axis. This reduces to three the possible irreducible representations compatible with the magnetic properties of these compounds. The magnetic structure of both compounds was then solved by trial and error using the Rietveld method implemented in FULLPROF (Rodríguez-Carvajal 1990, 1993). The irreducible representation that unambiguously describes the magnetic structure of both compounds is $\Gamma_{1u}(A_x, —, C_z)$. A simple group theoretical analysis leads to the $Pn'm'a'$ as the Shubnikov magnetic group associated with Γ_{1u} (Opechowski and Guccione 1965, Prandl 1978). The symmetry analysis is summarized in table 8.

The representation Γ_{1u} allows the magnetic moments to lie in the *ac* plane. However,

Table 8. Magnetic modes and magnetic space groups for Fe sites in *Pnma*. The generators of the factor group are: 2_{1z} $(\frac{1}{4}, 0, z)$, $2_{1y}(0, y, 0)$ and $-1(0, 0, 0)$. The label of the representations is $\Gamma_{nv}(c_1, c_2)$, where n is 1, 2, 3, 4, v is the character of the inversion centre, g or u (*gerade* or *ungerade*), and c_1, c_2 are the characters (+ or −) of generators 2_{1z} and 2_{1y}, respectively. The symbols F, G, A, C mean the following sequences of spin signs: $F(+ + ++)$; $G(+ - +-)$; $A(+ - -+)$; $C(+ + --)$. The four signs correspond to atoms numbered in the following order: $1(x, \frac{1}{4}, z)$; $2(-x + \frac{1}{2}, \frac{3}{4}, z + \frac{1}{2})$; $3(-x, \frac{3}{4}, -z)$ and $4(x + \frac{1}{2}, \frac{1}{4}, -z + \frac{1}{2})$.

Representation	Basis function			Shubnikov group
$\Gamma_{1g}(++)$	—	G_y	—	*Pnma*
$\Gamma_{2g}(+-)$	G_x	—	F_z	*Pn'm'a*
$\Gamma_{3g}(-+)$	—	F_y	—	*Pn'ma'*
$\Gamma_{4g}(--)$	F_x	—	G_z	*Pnm'a'*
$\Gamma_{1u}(++)$	A_x	—	C_z	*Pn'm'a'*
$\Gamma_{2u}(+-)$	—	A_y	—	*Pnma'*
$\Gamma_{3u}(-+)$	C_x	—	A_z	*Pn'ma*
$\Gamma_{4u}(--)$	—	C_y	—	*Pn'ma*

the fit of the experimental data from D1B (figure 3) to the magnetic structure described by Γ_{1u} reduces the m_z component of the magnetic moment to a null or negligible value in such a way that m_x is the only component of the magnetic moments, a fact that agrees with magnetic susceptibility data. The magnetic moments are therefore parallel and antiparallel to the direction of the a axis and form ferromagnetic planes perpendicular to the b axis. The orientation of these moments reverses when moving from an ac plane to the next one, so that the total ordering is antiferromagnetic (figure 4).

Knowledge of the magnetic structure can help to clarify the possible existence of piezomagnetism in these compounds. As mentioned in the introduction, piezomagnetism has been suggested as a possible origin of the low-field remanent magnetization observed in solid solutions of these materials (Kushauer *et al* 1994). The piezomagnetic effect consists in the appearance of a spontaneous magnetic moment under the application of stress to the material. However, several magnetic symmetries cannot support piezomagnetism. The piezomagnetic effect can only be exhibited by crystals belonging to 66 of the 90 total magnetic classes (Birss 1966). Since $m'm'm'$, the magnetic class of our crystals, is one of the 24 classes in which piezomagnetism is forbidden, it can be concluded that the piezomagnetic effect cannot occur in $K_2FeCl_5 \cdot D_2O$ and $Rb_2FeCl_5 \cdot D_2O$.

The cyclic magnetic structure refinement of the diffractograms collected on D1B allows us to determine the temperature dependence of the sublattice magnetization as shown in figure 5. The small tail observed in the magnetization curves as T approaches T_N is due to diffuse scattering indicating the presence of a certain lower dimensionality in these compounds. This is in good agreement with the dimensionality crossover from 1D to 3D in the Heisenberg lattice observed in these compounds (Puértolas *et al* 1985). The total magnetic moment found for each sublattice at 1.5 K is 3.9(1) μ_B and 4.06(5) μ_B for respectively the K and Rb compounds. This value is far below the value of 5 μ_B, expected for the saturated magnetic moment of an $S = \frac{5}{2}Fe^{3+}$ ion. Spin delocalization due to covalence in the Fe–Cl and the Fe–O bonds may be the most likely origin of the moment reduction at the iron sites. Similar reductions have been observed in other chlorinated systems: $FeCl_3$ (Stampfel *et al* 1973) and $Co(pn)_3FeCl_6$ (Scoville *et al* 1983). Polarized neutrons have been used as a probe of such a spin delocalization in other systems with

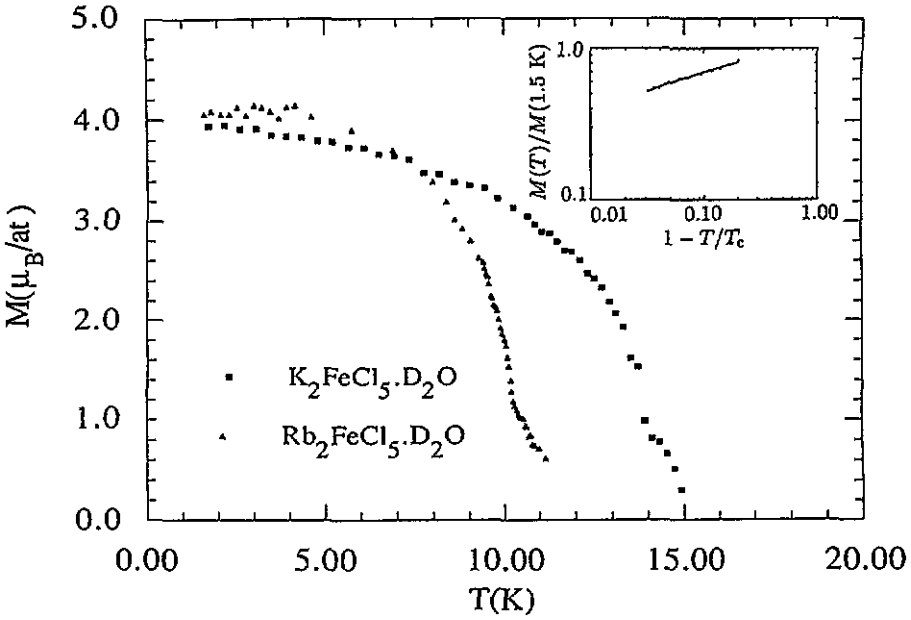

Figure 5. Temperature dependence of the sublattice magnetic moment for $Rb_2FeCl_5 \cdot D_2O$ and $K_2FeCl_5 \cdot D_2O$. The inset shows the log–log plot of $M(T)/M(1.5\ K)$ versus $1 - T/T_c$.

covalent bonding (Gillon *et al* 1989).

The temperature dependence of the sublattice magnetization shows minor differences for both compounds. In the critical region, it is expected to vary as $M(T)/M(0) = B(1 - T/T_c)^{\beta}$. From a log–log plot of $M(T)/M(1.5\ K)$ versus $1 - T/T_N$, a β value of 0.35 ± 0.02 can be deduced for the Rb compound in the reduced temperature range $0.03 \leqslant 1 - T/T_c \leqslant 0.2$ (inset figure 5). The β value is in excellent agreement with the theoretical value of 0.36 predicted for a three-dimensional Heisenberg antiferromagnet (de Jongh and Miedema 1974). There are some difficulties in extending the temperature range of $M(T)$ to values of $1 - T/T_c$ lower than 10^{-2}. As one approaches T_N, the Bragg scattering rapidly decreases while the diffuse critical scattering becomes stronger. This gives a large uncertainty to the determination of the sublattice magnetization in the region very close to T_N. The same analysis cannot be made on the K derivative because of the smaller number of experimental data points available in the critical region. However, a rather similar value should be expected for β, due to the close analogy of this compound with the Rb derivative. The value of the β exponent found here compares well with that corresponding to other three-dimensional Heisenberg antiferromagnets. A β value of 0.32 ± 0.02, determined in the temperature range $8.4 \times 10^{-4} \leqslant t \leqslant 1.3 \times 10^{-2}$, has been reported for $RbMnF_3$ by Tucciarone and co-workers using elastic neutron scattering (Tucciarone *et al* 1971), while Heller observed a $\beta = 0.335 \pm 0.005$ for the more anisotropic compound MnF_2 from NMR measurements in the reduced temperature range $7 \times 10^{-5} \leqslant t \leqslant 8 \times 10^{-2}$ (Heller 1966).

4. Conclusions

Refinement of the nuclear structures of $K_2FeCl_5 \cdot D_2O$ and $Rb_2FeCl_5 \cdot D_2O$ from neutron powder diffraction experiments at 20 K indicates the absence of crystallographic phase transitions from the structures at room temperature. The refinement also defines the position

of the hydrogen bonds that are believed to play an important role in the transmission of the superexchange magnetic interactions on these compounds.

The determination of the magnetic structure indicates that the magnetic moments of the iron atoms are parallel and antiparallel to the direction of the a axis and form ferromagnetic planes perpendicular to the b crystallographic axis. The structure is well described by the irreducible representation $\Gamma_{1u}(A_x,—,C_z)$ of the *Pnma* space group for $k = (0, 0, 0)$ which corresponds to the $Pn'm'a'$ Shubnikov magnetic group. This group belongs to the magnetic class $m'm'm'$ in which piezomagnetism is not allowed.

The temperature dependence of the staggered magnetization curve, as calculated from cycling refinement of neutron diffraction patterns, gives an anomalously low value for the saturation magnetization. Although no definitive explanation has been found for such a reduction in the magnetic moment of the iron atoms, the possibility of spin delocalization through covalent bonding is suggested. The fitting of the magnetization curve corresponding to the Rb derivative to a critical law yields a value of 0.35 ± 0.02 for the critical exponent β, in good agreement with the theoretical predictions for a 3D Heisenberg lattice.

Acknowledgments

The authors are grateful to Milagros Tomás for her assistance with x-ray measurements. We are also gratefully indebted to M Carmen Morón and Domingo González for many helpful discussions. The research has been supported by grants MAT91-681 and MAT94-0043 from the Comisión Interministerial de Ciencia y Tecnología. DV thanks the British Council and SERC for financial support.

References

Becerra C C, Paduan-Filho A, Fries T, Shapira Y and Palacio F 1994 *J. Phys.: Condens. Matter* **6** 5725–40
Bellanca A 1948 *Periodico Mineral.* XVII 59–72
Bertaut E F 1968 *Acta Crystallogr.* A **24** 217–31
Birss R R 1966 *Symmetry and Magnetism* ed E P Wohlfarth (Amsterdam: North-Holland)
Borovik-Romanov A S 1960 *Sov. Phys.–JETP* **11** 786–93
Carlin R L and Palacio F 1985 *Coord. Chem. Rev.* **65** 141–65
de Jongh L and Miedema A R 1974 *Adv. Phys.* **23** 1–260
Erickson R A 1953 *Phys. Rev.* **90** 779–85
Fries T, Shapira Y, Paduan-Filho A, Becerra C C and Palacio F 1993a *J. Phys.: Condens. Matter* **5** L107–12
——1993b *J. Phys.: Condens. Matter* **5** 8083–96
Gillon B, Cavata C, Schweiss P, Journaux Y, Kahn O and Schneider D 1989 *J. Am. Chem. Soc.* **111** 7124–32
Heller P 1966 *Phys. Rev.* **146** 403–22
Johnson J A, Johnson C E and Thomas M F 1987 *J. Phys. C: Solid State Phys.* **20** 91–109
Kushauer J, Kleeman W, Mattsson J and Nordblad P 1994 *Phys. Rev.* B **49** 6346–9
Lederman M, Hammann J and Orbach R 1990 *Physica* B **165 & 166** 179–80
Linke W F 1965 *Solubilities of Inorganic and Metal Organic Compounds* 4th edn, vol I (Washington, DC: American Chemical Society)
McElearney J N and Merchant S 1978 *Inorg. Chem.* **17** 1207–15
O'Connor C J, Bascom S D Jr and Sinn E 1979 *J. Chem. Phys.* **70** 5161–7
Opechowski W and Guccione R 1965 *Treatise on Magnetism* vol IIA, ed H Suhl and G Rado (New York: Academic)
Paduan-Filho A, Barbeta V B, Becerra C C, Gabás M and Palacio F 1992 *J. Phys.: Condens. Matter* **4** L607–10
Palacio F, Gabás M, Campo J, Becerra C C, Paduan-Filho A, Fries T and Shapira Y 1994 *Phys. Scr.* T **55** 163–6
Palacio F, Paduan-Filho A and Carlin R L 1980 *Phys. Rev.* B **21** 296–8
Palacio F and Visser D 1995 to be published
Prandl W 1978 *Neutron Diffraction* ed H Dachs (Berlin: Springer)
Puértolas J A, Navarro R, Palacio F, Bartolomé J, González D and Carlin R L 1982 *Phys. Rev.* B **26** 395–403
——1985 *Phys. Rev.* B **31** 516–26

Rodríguez-Carvajal J 1990 *Abstracts Satellite Meeting XVth Congr. Int. Union Crystallogr. (Toulouse)*
——1993 *Physica* B **192** 55–69
Schultz A J and Carlin R L 1995 *Acta Crystallogr.* B **51** 43–7
Scoville A N, Lázár K, Reiff W M and Landee C 1983 *Inorg. Chem.* **22** 3514–9
Solans X, Morón M C and Palacio F 1988 *Acta Crystallogr.* C **44** 965–7
Stampfel J P, Oosterhuis W T, Window B and de S Barros F 1973 *Phys. Rev.* B **8** 4371–82
Tucciarone A, Lau H Y, Corliss L M, Delapalme A and Hastings J M 1971 *Phys. Rev.* B **4** 3206–44
Wignacourt J P, Mairesse G and Barbier P 1976 *Cryst. Struct. Commun.* **5** 293–6